

Received: 2018.12.11  
Accepted: 2019.02.04  
Published: 2019.02.18

# miR-193a-3p Promotes Radio-Resistance of Nasopharyngeal Cancer Cells by Targeting SRSF2 Gene and Hypoxia Signaling Pathway

Authors' Contribution:  
Study Design A  
Data Collection B  
Statistical Analysis C  
Data Interpretation D  
Manuscript Preparation E  
Literature Search F  
Funds Collection G

ABE 1,2 **Lingsuo Kong**  
C 2 **Qing Wei**  
D 3 **Xianwen Hu**  
F 2 **Lauren Chen**  
AG 1,4 **Juan Li**

1 Shandong University Medical College, Ji'nan, Shandong, P.R. China  
2 Department of Anesthesiology, West Branch of The First Affiliated Hospital of University of Science and Technology of China, Ji'nan, Shandong, P.R. China  
3 Department of Anesthesiology, The Second Affiliated Hospital of Anhui Medical University, Hefei, Anhui, P.R. China  
4 Department of Anesthesiology, South Branch of The First Affiliated Hospital of University of Science and Technology of China, Hefei, Anhui, P.R. China

**Corresponding Author:** Juan Li, e-mail: huamuzi1999@163.com

**Source of support:** This study was supported by the First Group of Science and Technology Project of Anhui Province (1503062021), granted to JL

**Background:** Radio-resistance is an important barrier in nasopharyngeal carcinoma treatment. MicroRNAs are gene expression core regulators in various biological procedures containing cancer radio-resistance. Nevertheless, the clinical association between nasopharyngeal carcinoma and miR-193a-3p/SRSF2 remains unclear.

**Material/Methods:** We examined the miR-193a-3p level in radio-sensitive CNE-2 and radio-resistant CNE-1 NPC cell lines, and, based on a literature review, predicted SRSF2 to be the target gene of miR-193a-3p. We explored the expression of SRSF2 at protein and mRNA levels by transfecting either miR-193a-3p-mimic or antagomiR. Finally, we performed signaling pathway analysis to assess the possible role of miR-193a-3p/SRSF2 in signaling pathways.

**Results:** miR-193a-3p promotes NPC radio-resistance, and the SRSF2 gene is the direct target for miR-193a-3p in NPC, and thus is negatively correlated with NPC radio-resistance. The hypoxia signaling pathway activity is strongly affected, and it is possible to use the downstream activity of the SRSF2 gene to show the effect of miR-193a-3p on radio-resistance in NPC cells.

**Conclusions:** miR-193a-3p mediates promotion of NPC radio-resistance.

**MeSH Keywords:** **Head and Neck Neoplasms • Nasopharyngeal Diseases • Nasopharyngeal Neoplasms**

**Abbreviations:** **NPC** – nasopharyngeal carcinoma; **miR** – microRNA; **WT** – pGL3-SRSF2 UTR wild-type; **UTR** – untranslated region; **3PM** – miR-193a-3p mimic; **3PA** – miR-193a-3p antagomiR; **MT** – pGL3-SRSF2 UTR mutant; **Vec** – pGL3 enhancer control

**Full-text PDF:** <https://www.basic.medscimonit.com/abstract/index/idArt/914572>

 2555

 1

 5

 30



## Background

Nasopharyngeal carcinoma (NPC) is a neoplastic disorder that arises from the lining of the nasopharynx. NPC is most common in Southeast Asia and Southern China, and it is one of the leading malignancies with obscure etiology [1]. Radio-therapy is an important treatment for non-metastatic NPC. The combination of radio-therapy with chemotherapy can increase survival, even in relatively advanced NPC [2]. However, due to the radio-resistance, some NPC patients treated with radio-therapy have local recurrences and distant metastases after 1–2 years [3]. Therefore, it is important to identify the related genes and define the potential mechanisms for the improvement of radio-resistance of NPC.

MicroRNAs (miRNA) belong to a class of conserved endogenous non-coding small RNAs, which are involved in a wide range of biological processes [4]. They are identified as potential cancer biomarkers and are related to distinct tumor behaviors, including proliferation [5], invasion [6], metastasis [7], angiogenesis [8], and chemoresistance [9]. Aberrant expression of miRNAs, such as miR-210, miR-32, miR-21, and miR-7, is involved in the radio-resistance of multiple cancers [10–13]. Of note, several miRNAs were found to regulate the radio-resistance of NPC, such as miR-324-3p [14], miR-185-3p [15], and miR-205 [16]. Among the miRNAs that have been studied, dysregulation of miR-193a-3p has been reported in colorectal cancer [17], breast cancer [18], and prostate cancer [19]. miR-193a-3p has also been reported to be involved in multi-drug-resistant bladder cancer [20]. Nevertheless, the role of miR-193a-3p in response to radiation treatment for NPC is unclear.

SRSF2 is a 35 kDa serine/arginine-rich protein, which belongs to the highly conserved splicing factor family in higher eukaryotes, contributing to gene splicing and alternative splicing. SRSF2 plays a key role in additional interactions between the various steps in expression of the SRSF2 gene, and can also regulate transcriptional activation and elongation [21]. By interacting with transcription factor E2F1, SRSF2 stimulation regulates cell cycle gene activity [22]. SRSF2 not only changes the splicing mode, but also changes the expression of genes involved in apoptosis [23].

In the present study, we assessed genes that are differentially expressed in NPC. We found that NPC radio-resistance is facilitated by miR-193a-3p through SRSF2 gene repression, which is a recently identified miR-193a-3p target. We performed a systematic analysis of role of the SRSF2 gene in NPC cell radio-resistance.

## Material and Methods

### Cell lines

We used the cells lines of human nasopharyngeal carcinoma, including radio-sensitive CNE-2 and radio-resistant CNE-1 [24]. Cells were cultured in RPMI medium 1640 with 10% fetal bovine serum (Invitrogen, CA, America) in 5% CO<sub>2</sub> at room temperature.

### Transient transfection assays

The si-SRSF2, scrambled negative control (NC), antagomiR, and *Homo sapiens* miR-193a-3p mimics were from Ribobio (Guangzhou, China). AntagomiR and miR-193a-3p mimics were designed for overexpressing and suppressing the expression of miR-193a-3p, respectively. si-SRSF2 was adopted for decreasing SRSF2 expression. Transient transfection was performed according to the manufacturer's instructions.

The sequences were:

antisense 5'-ACUGGGACUUUGUAGGCCAGUU-3'

sense 5'-AACUGGCCUACAAAGUCCAGU-3'

mimics:

antagomiR: 5'-ACUGGGACUUUGUAGGCCAGUU-3';

hsa-miR-193a-3p

hi-SRSF2:

5' UCGGUCUCCAGAUCUCGUUTT 3'

5' AACGAGAUCUGGAGACCGATT 3'

### Reverse transcription-quantitative polymerase chain reaction (qRT-PCR) assays

In accordance with the instructions of the manufacturer, the overall RNA was extracted by TRIzol reagent (Invitrogen, USA). The PCR primers and reverse-transcription for U6 and miR-193a-3p were from Ribobio (Guangzhou, China). The cDNA library was synthesized. The mRNA expression level of SRSF2 was assessed by TaqMan assay and miRNA using SYBR Green assay (Biosystems, CA, America) quantified with an FTC-3000PCR instrument (Funglyn Biotech, Inc., Canada). Either β-actin or U6 small nuclear RNA (HmiRQP9001) (ShingGene, Shanghai, China) was used as an internal control [25]. Expression levels were measured using the related quantification strategy (2<sup>-ΔΔCt</sup>). All tests were repeated in triplicate.

### Radiation exposure and clonogenic assays

Every cell was pretreated by si-SRSF2, antagomiRs, miR-193a-3p mimics, and NC for 24 h and then seeded onto 6-well plates in triplicate, followed by exposure to 0, 2, 4, 6, or 8 Gy radiation. After being incubated for 10–14 days at room temperature, colonies were stained by using crystal violet, and colonies with over 50 cells were counted. The colony-formation

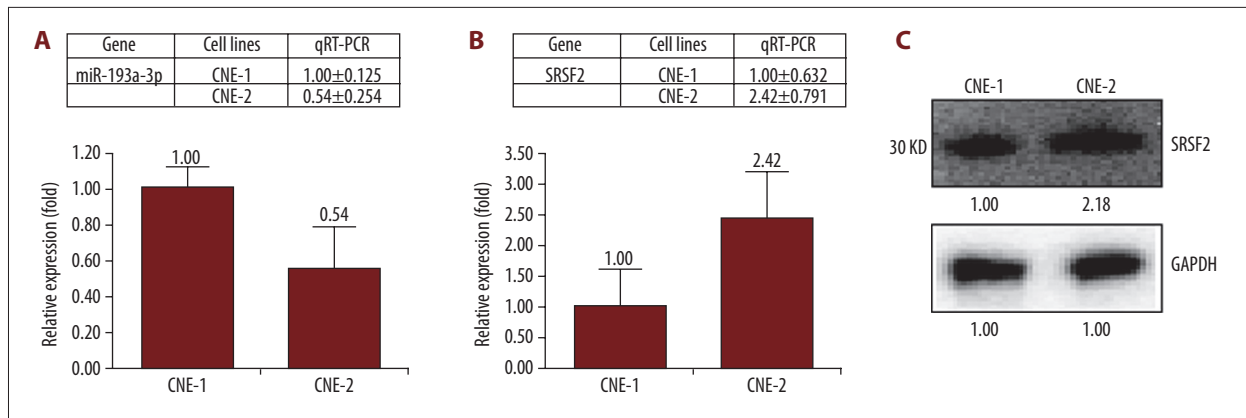


**Figure 1.** (A–C) Expression of miR-193a-3p/SRSF2 within radio-sensitive CNE-2 and radio-resistant CNE-1 nasopharyngeal cells. The expression levels of miR-193a-3p within CNE-2. SRSF2 expression level was higher within CNE-2 cells compared with that in CNE-1 cells, as shown in Table B. Western blot and qRT-PCR analyses results are presented in plot C.

effectiveness was assessed by the average number of plated cells. The multi-target single-hit pattern was fit to the statistics for generating survival fraction (SF) by use of the equation:  $SF = 1 - (1 - e^{-D/D_0})^N$ . The parameters SF2, D0, Dq, and N were calculated. More than 3 separate tests were conducted.

#### Western blotting assays

Protein were extracted from cells at exponential development stage by use of a lysis buffer, transferred to a PVDF membrane from the gel, and separated by 10% SDS-PAGE. Later, the PVDF membrane was blocked with 5% non-fat milk. Then, the primary antibodies were detected by second antibodies. Anti-GAPDH, anti-mouse, anti-rabbit, and SRSF2's rabbit polyclonal antibodies were purchased from HopeBiot (cat. no. PR-8305), and the concentration was 45 µg/150 µl. The target bands were visualized and the related band intensity was assessed.

#### Apoptosis assays

Transfected and parental (2 days) cells within the log growth phase were harvested and washed twice using PBS, then 5 µl (20 µg/ml) of propidium iodide-labeled necrosis factor and 5 µl of Annexin V-FITC-labeled apoptosis factor were added to 200 µl of cell suspension. Then, the cells were incubated for 30 min in the dark at room temperature, and apoptosis was quantified using a FACSCalibur flow cytometer (Beckman Coulter, USA) and analyzed by Flowjo7.6 software (TreeStar, San Carlos, CA, USA). Every test was performed in triplicate and a representative result is presented.

#### Luciferase reporter assays

The mutant (MT) 3'UTRs and SRSF2 wild-type (WT), including the putative miR-193a-3p binding site, were cloned to the PGL3-luciferase-report vector (Invitrogen, USA). For luciferase

reporter assay, CNE-2 and CNE-1 cells were co-transfected with the antagomiR or miR-193a-3p mimic. After transfection for 24 h, the cells were assayed for luciferase activity, in accordance with the instructions of the manufacturer. All tests were repeated in triplicate.

#### Signaling pathway analysis

Concepts for Constructs for 18 signaling pathway reporters were from SA Biosciences (USA) and were used according to the manufacturer's instructions. The cells were transfected in triplicate, with every firefly luciferase reporter construct calculated within the cell extracts after transfection for 24 h. The pathway reporter luciferase activities (luciferase unit) were used to indicate pathway activity relative to the negative control.

#### Wound-healing assays

For motility assays, cells were grown to near confluence. The cell layer was scratched by using a 10-µl sterile pipette tip and washed extensively with PBS to remove cellular debris. Cells were then incubated in medium with 10% FBS. The injured region was measured and photographed at 0, 8, 24, and 48 h after scratching. All tests were repeated in triplicate.

#### Transwell invasion assays

The Transwell cell invasion experiment was carried out on 24-well plates with a pore size of 8 µm. In the invasion experiment,  $1 \times 10^4$  cells with stable expression of mimics or NC were placed in the upper chamber, and the matrix gel coating membrane was diluted in serum-free medium. In the experiment, cells were suspended in 100 µl RPMI-1640 without FBS and then inoculated into the upper chamber. In the lower chamber, we added 500 µl RPMI-1640 and 10% FBS. After 30 h of incubation, the inserts were removed from the culture plate

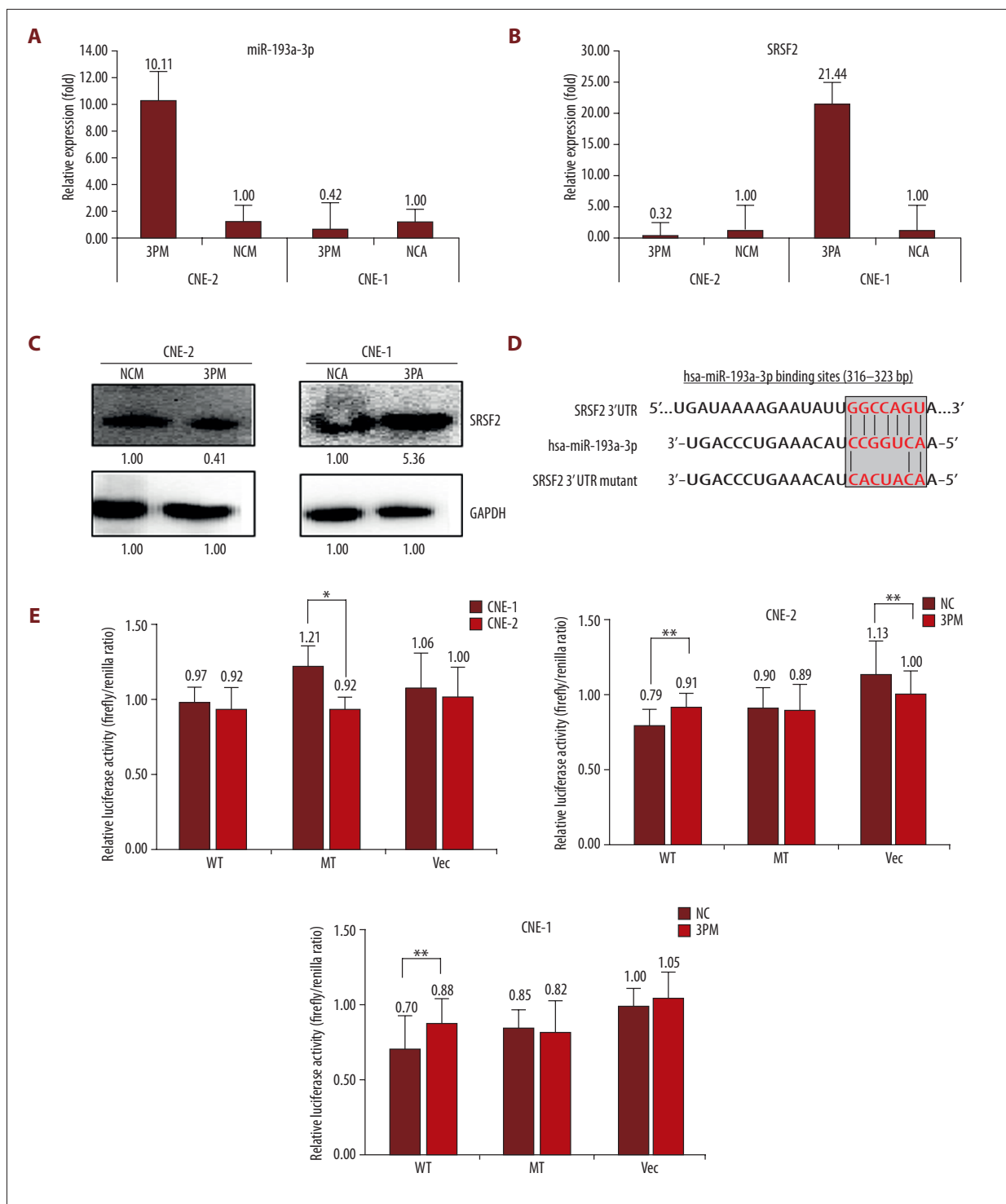


**Figure 2.** SRSF2 is a direct target of miR-193a-3p within NPC cells. SRSF2 mRNA, miR-193a-3p, and protein levels within the CNE-1 cells, as well as miR-193a-3p mimic (3PM)-transfected CNE-2 cells, were assessed by Western blot analyses (C) or qRT-PCR (A, B). Sequences within the UTR area of SRSF2 gene are targeted by miR-193a-3p. Cross-hatching shows the synthetic region (D). The reporter's related luciferase activities (fold) without the UTR (Vec) or with the wild-type (WT) SRSF2-UTR were assessed within the NPC cells transfected with the antagonomiR (in CNE-1), miR-193a-3p mimic (in CNE-2), or Mock (E) sequences. Renilla luciferase activity of Aco-transfected control plasmid was used a control for the effectiveness of the transfection. \* p value<0.05 by t test.

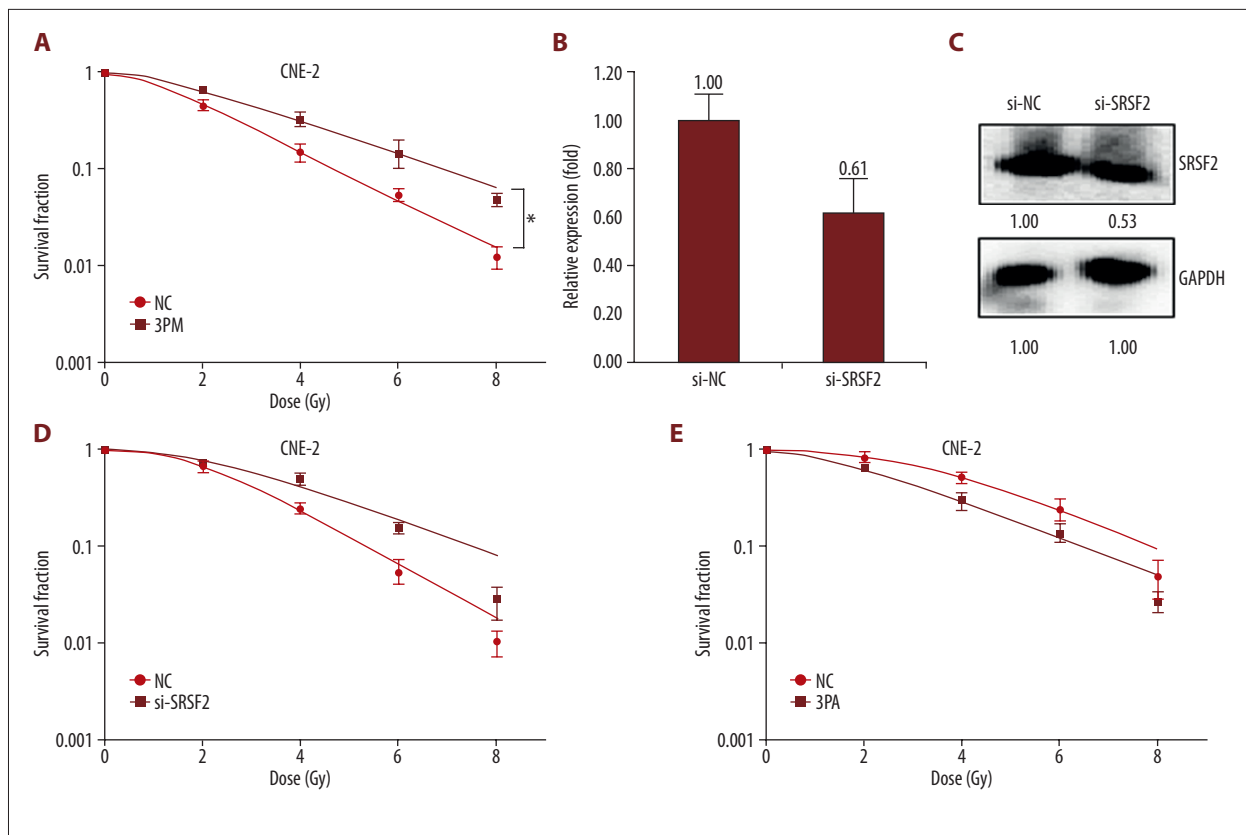


**Figure 3.** Effect of forced reversal of SRSF2 or miR-193a-3p levels on CNE-2 and CNE-1 cell radio-resistance. The survival fraction of NC cells is increased by miR-193a-3p mimic (3PM)-transfected CNE-2 against the negative control (NC) cells (A). The protein (Western blot analysis) and SRSF2 mRNA (qRT-PCR) levels within the si-SRSF2-transfected against the NC-transfected CNE-2 cells treated with a 4-Gy dose of radiation (B, C). The survival fraction of NC cells was increased by Si-SRSF2-transfected CNE-2 against the negative control (NC) cells (D) and were reduced by miR-193a-3p antagomiR (3PA)-transfected CNE-1 against the negative control (NC) cells (E). The survival fraction was determined using the multi-target single-hit pattern:  $Y=1-(1-\exp(-k*x))^N$ . The mean  $\pm$  the outcome standard deviation from 3 independent tests.

and the non-invasive cells were removed from the surface of the membrane. Cells moving to the bottom of the chamber were stained with 0.1% crystal violet for 30 min. The cells were then imaged and counted using a CKX41 inverted microscope in at least 5 randomly selected areas. Three independent tests were carried out.

### Statistical analyses

The results are shown as mean  $\pm$  standard deviation. All statistical analyses were performed using GraphPad Prism and Excel. Two-way ANOVA and two-tailed *t* test were used to calculate statistical significance, with  $p < 0.05$  considered statistically significant.

## Results

### The SRSF2 level negatively correlates with the expression of miR-193a-3p in NPC cells

CNE-2 and CNE-1 are the radio-sensitive and radio-resistant cell lines, respectively of NPC [24]. To explore the mechanism regulating NPC cell radio-resistance, miR-193a-3p was chosen as the target because it was previously reported to have great significance in bladder cancer chemotherapeutics in our earlier study [25,26]. miR-193a-3p expression was further detected through qRT-PCR assay. The RT-PCR analysis outcomes show that miR-193a-3p expression is 0.54-fold higher within the CNE-1 cells than within the CNE-2 cells (Figure 1A).

The target gene expression is often suppressed by a given miRNA, thereby regulating the pathways. The miR-193a-3p target genes were predicted based on our earlier study, showing that the SRSF2 gene levels are significantly differentially

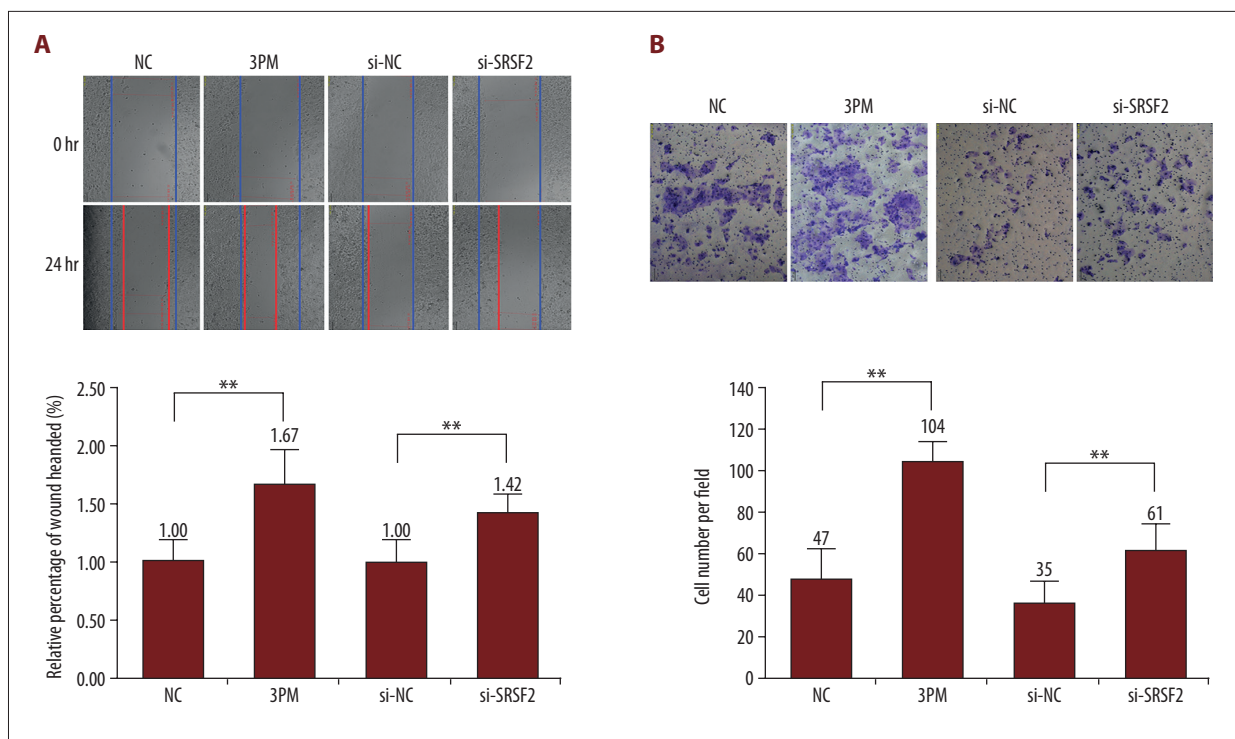


**Figure 4.** Wound-healing and invasion assays, in which the invasion and migration abilities of CNE-2 cell were assessed with transient expression of the si-SRSF2 and miR-193a-3p mimic (3PM) (A, B). Results of 3 separate tests. \*\*  $p < 0.01$ ; \*  $p < 0.05$  by *t* test. (Magnification: 40 $\times$ ).

expressed and are negatively correlated with miR-193a-3p expression. The SRSF2 expression level was 2.42-fold lower in CNE-1 cells than in CNE-2 cells, as determined by qRT-PCR (Figure 1B). The subsequent Western blot analysis also suggested a higher level of SRSF2 in CNE-2 cells than in CNE-1 cells (Figure 1C). The lower expression of SRSF2 in radio-resistant CNE-1 cells suggests SRSF2 is a negative regulator of NPC radio-resistance.

#### The SRSF2 gene is a direct target of miR-193a-3p in NPC cells

The miR-193a-3p level was lower in CNE-2 cells than in CNE-1 cells, which may correlate negatively with the SRSF2 levels. To determine if SRSF2 is a target of miR-193a-3p, the SRSF2 level was assessed within the miR-193a-3p mimic (3PM)-transfected CNE-2 and the antagomiR (3PA)-transfected CNE-1 cells against transfection of NC. The transfection of miR-193a-3p mimic into CNE-2 cells increased its expression by nearly 10-fold (Figure 2A), while miR-193a-3p antagomiR transfection into CNE-1 cells reduced its level to 42% (Figure 2A). Following the miR-193a-3p level changes, the transfection of miR-193a-3p mimic decreased the proteins to almost 41% and SRSF2 mRNA to 32% (Figure 2B, 2C) compared with that within the NC-transfected CNE-2 cells. The mRNA level and the protein level of SRSF2 were increased by 21.44-fold by transfection

of miR-193a-3p antagomiR (Figure 2B) and by 5.36-fold within CNE-1 cells (Figure 2C).

Sequence analysis indicated the 3'UTR area of SRSF2 includes an underlying binding motif for miR-193a-3p (Figure 2D). To further assess if SRSF2 is a direct target of miR-193a-3p, the mutant or wild-type SRSF2 UTR was put downstream of the pGL3-control vector's Renilla luciferase gene (Promega) (Figure 2D). The pGL3 enhancer control (Vec), mutant (MT), and pGL3-SRSF2 UTR wild-type (WT) were transfected into CNE-1 and CNE-2 cells, respectively, to determine if the miR-193a-3p, which was expressed differentially within NPC cells, is actually functional. The luciferase activities of 0.92 and 0.97 were shown by the pGL3-SRSF2-UTR WT within CNE-2 and CNE-1 cells, respectively, and that of 0.92 and 1.21 for the MT (Figure 2E). The pGL3-SRSF2-UTR WT construct's luciferase activity was increased by 3PM's transfection into CNE-2 cells (Figure 2E), while the MT and control cells presented nearly the same activity on 3PM transfection (Figure 2E). GL3-SRSF2-UTR WT construct luciferase activity was raised by 3PA transfection into the CNE-1 cells (Figure 2E), whereas the MT and Vec cells showed no significant difference after transfection of 3PA. In conclusion, SRSF2 appears to be a direct target of miR-193a-3p and may be the mechanism by which miR-193a-3p promotes the effect on radio-resistance in NPC.

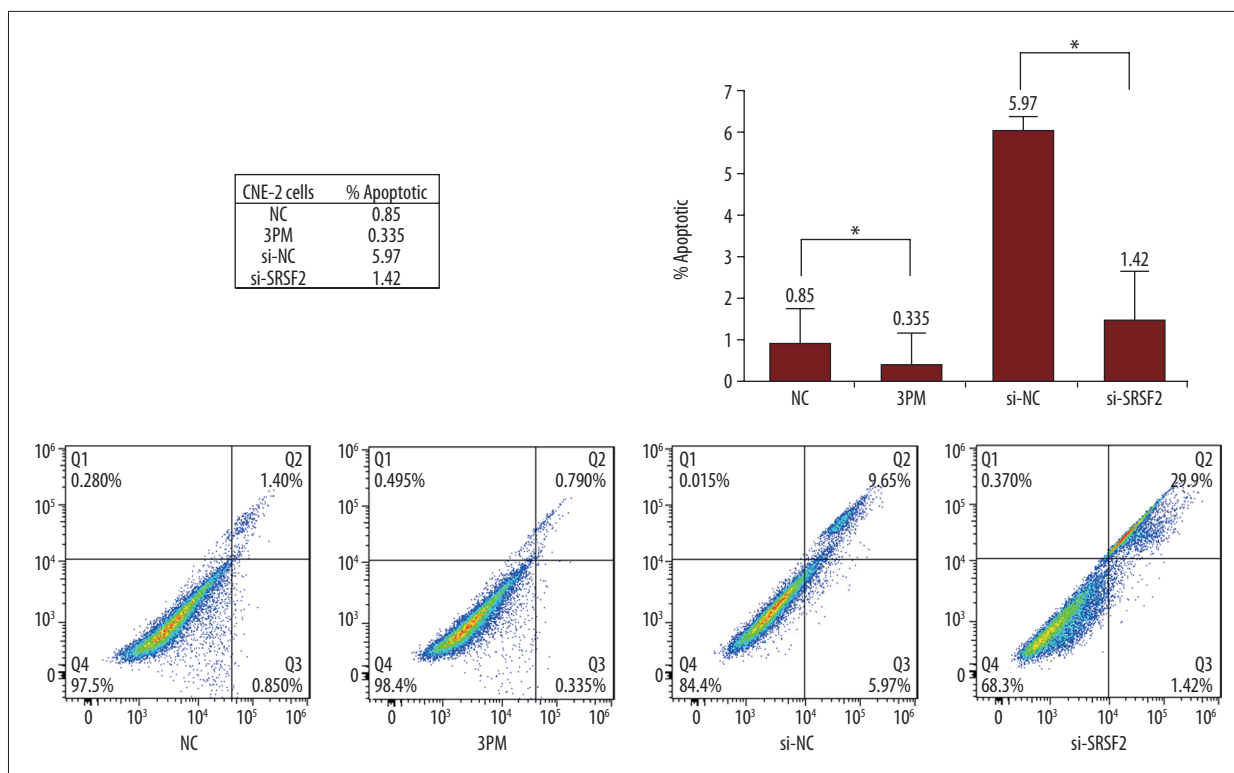


**Figure 5.** Effects of forced reversal of SRSF2 and miR-193a-3p levels on the CNE-1 cell apoptosis, with a graph of the discussed statistics, as well as the plots of the primary FACS resources. \*  $p < 0.05$ .

### The SRSF2 expression is negatively correlated with miR-193a-3p's promoting effect on NPC radio-resistance

To explore the role of SRSF2 in the radio-resistance of NPC, 3PM was first transfected into CNE-2 cells and the miR-193a-3p level was examined. The miR-193a-3p level was increased by 3PM's transfection in the CNE-2 cells. Accompanied by increased miR-193a-3p, the survival rate of cells exposed to radiation treatment was increased (Figure 3A). Subsequently, si-SRSF2 was transfected into CNE-2 cells and the effect of radiation treatment was assessed. The level of SRSF2 was decreased by si-SRSF2 transfection into CNE-2 cells at mRNA (0.61: 1.00) and protein levels (0.53: 1.00), in comparison to control cells (Figure 3B, 3C). As a result, CNE-2 cell radio-resistance was been increased with si-SRSF2 transfection (Figure 3D), in accordance with miR-193a-3p's reverse effect. Additionally, 3PA was transfected into CNE-1 cells to decrease the miR-193a-3p level, which reduced the survival rate of cells exposed to radiation treatment (Figure 3E). These outcomes are in agreement with SRSF2's negative regulation in radio-resistant NPC. In summary, the SRSF2 gene appears to be involved in promoting radio-resistance of NPC by miR-193a-3p.

### miR-193a-3p enhances cell migration and invasion of NPC cells

The invasion and migration abilities of CNE-2 and CNE-1 cells was further compared by invasion and wound-healing assays, respectively. The migration ability was significantly increased compared with the control cells by transfection of either si-SRSF2 or 3PM into CNE-2 cells (Figure 4A). In the same manner, the invasion ability was also increased by transfection of either si-SRSF2 or 3PM into CNE-2 cells (Figure 4B).

In line with the ability of miR-193a-3p to promote invasion and migration of cells, the cell apoptosis rate was decreased to 0.335% from 0.85%, which indicated an increased survival rate of cells (Figure 5). A similar effect was also found in the si-SRSF2-transfected CNE-2 cells, which resulted in a reduction of cells from 5.97% to 1.42% (Figure 5).

### miR-193a-3p regulates activities of the hypoxia signaling pathway in the context of NPC radio-resistance

To understand the molecular mechanisms involved in miR-193a-3p-regulated NPC radio-resistance, CNE-2 and CNE-1 cells were to measure the activities of a series of signaling pathways related to cancer (Table 1A). We selected 3 pathways – Notch, hypoxia, and MEF2 – that were over 10-fold

**Table 1.** The signaling pathways are regulated by miR-193a-3p as well as its downstream genes. The relative activities (mean  $\pm$ S.D.) of the 3 pathways which are different (A). The pathways' relative activities within the miR-193a-3p mimic (3PM)-transfected against NC-transfected CNE-2 cells and miR-193a-3p antagomiR (3PA)-transfected against NC-transfected CNE-1 cells (B). The pathways' relative activities within the si-SRSF2-transfected against NC-transfected CNE-2 cells as well as GFP-SRSF2-transfected against NC-transfected CNE-1 cells (C).

(A) Pathway	Transcription Factor	CNE-1	CNE-2	CNE-1/CNE-2
Wnt	TCF/LFC	2.416	1.172	2.061
Notch	RBP-J $\kappa$	4.382	105.409	0.042
P53/DNA damage	p53	2.072	1.884	01.100
TGF $\beta$	SMAD2/3/4	6.318	2.229	2.834
Cell cycle/pRb-	E2F/DP1	3.776	2.596	1.454
NF $\kappa$ B	NF $\kappa$ B	503.440	526.807	0.956
Myc/Max	Myc/Max	106.406	18.179	5.853
Hypoxia	HIF1A	736.080	28.362	25.953
MAPK/ERK	Elk-1/SRF	410.334	229.784	1.786
MAPK/JNK	AP-1	364.90	531.716	0.685
ATF2/ATF3/ATF	ATF2/ATF3/ATF4	227.761	44.187	5.154
cAMP/PKA	CREB	188.455	144.501	1.304
MAPK/JNK	FOS/JUN	371.718	524.434	0.709
MEF2	MEF2	2.114	899.307	0.002
Hedgehog	GLI	1.179	74.730	0.016
PI3K/AKT	FOXO	0.734	0.640	1.147
IL-6	STAT3	13.292	4.605	2.887
PKC/Ca $^{++}$	NFAT	0.986	1.054	0.936
Negative Control		1.000	1000	1000

(B) Pathway	Transcription factor	CNE-1		CNE-2	
		NC	3PA	NC	3PM
Notch	RBP-J $\kappa$	1.00 $\pm$ 0.21	0.61 $\pm$ 0.25	1.00 $\pm$ 0.41	1.85 $\pm$ 0.63
Hypoxia	HIF1A	1.00 $\pm$ 0.22	0.92 $\pm$ 0.11	1.00 $\pm$ 0.13	3.25 $\pm$ 0.54
MEF2	MEF2	1.00 $\pm$ 0.41	1.55 $\pm$ 0.47	1.00 $\pm$ 0.27	0.54 $\pm$ 0.17

(C) Pathway	Transcription factor	CNE-2	
		NC	Si-SRSF2
Notch	RBP-J $\kappa$	1.00 $\pm$ 0.11	2.76 $\pm$ 0.31
Hypoxia	HIF1A	1.00 $\pm$ 0.30	4.25 $\pm$ 0.14
MEF2	MEF2	1.00 $\pm$ 0.22	4.84 $\pm$ 0.18

higher in CNE-2 and CNE-1 cells. The MEF2 and Notch pathways presented lower activities in CNE-1 cells in comparison with those in CNE-2 cells, while the hypoxia pathway showed lower activities (Table 1). We then compared activities in the 3 pathways in 3PA-transfected CNE-1 cells or 3PM-transfected CNE-2

cells. Two pathways – MEF2 and hypoxia – were strongly correlated with altered miR-193a-3p levels in CNE-1 cells (Table 1). The activities of these 3 pathways were further compared in the GFP-SRSF2-overexpressed CNE-1 cells and si-SRSF2-transfected CNE-2 cells. Only the hypoxia pathway was correlated

with altered level of SRSF2 (Table 1). Therefore, only the hypoxia pathway was significantly correlated with altered expression of SRSF2 and miR-193a-3p.

## Discussion

Previous research showed that miRNAs participate in tumor radiosensitivity through regulation of various processes [28-29]. The significant roles of miRNAs in regulating diverse oncogenic processes, including radio-resistance, may promote better understanding of radiation resistance.

SRSF2 regulates transcriptional activation and extension, and stimulates gene-regulated cell cycle activity by interacting with transcription factor E2F1 [22]. In addition, SRSF2 mediates P-TEFb kinase recruitment and subsequently phosphorylates ser2 in the C-terminal domain of RNA polymerase II to promote transcriptional extension. SRSF2 can also enhance the stability of RNA. It is worth noting that the cell effects of SRSF2 depend on cell type and development stage, and srsf2 regulates transcriptional extension in a gene-specific manner. SRSF2 not only participates in the regulation of apoptosis by altering splicing mode, but also by altering the expression of apoptotic genes [30].

## References:

1. Yan XJ, Fang S, Huang GW et al: [Clinical study of nasopharyngeal masses with suspicion of nasopharyngeal carcinoma in adult patients]. *Zhonghua Er Bi Yan Hou Tou Jing Wai Ke Za Zhi*, 2018; 53: 519-23 [in Chinese]
2. DeNittis AS, Liu L, Rosenthal DI, Machtay M: Nasopharyngeal carcinoma treated with external radiotherapy, brachytherapy, and concurrent/adjuvant chemotherapy. *Am J Clin Oncol*, 2002; 25: 93-95
3. Guo Y, Zhu XD, Qu S et al: Identification of genes involved in radioresistance of nasopharyngeal carcinoma by integrating gene ontology and protein-protein interaction networks. *Int J Oncol*, 2012; 40: 85-92
4. Pillai RS, Bhattacharyya SN, Filipowicz W: Repression of protein synthesis by miRNAs: How many mechanisms? *Trends cell Biol*, 2007; 17: 118-26
5. Li T, Lu YY, Zhao XD et al: MicroRNA-296-5p increases proliferation in gastric cancer through repression of Caudal-related homeobox 1. *Oncogene*, 2014; 33: 783-93
6. Bockhorn J, Yee K, Chang YF et al: MicroRNA-30c targets cytoskeleton genes involved in breast cancer cell invasion. *Breast Cancer Res Treat*, 2013; 137: 373-82
7. Bouyssou JM, Manier S, Huynh D et al: Regulation of microRNAs in cancer metastasis. *Biochim Biophys Acta*, 2014; 1845: 255-65
8. Kong W, He L, Richards EJ et al: Upregulation of miRNA-155 promotes tumour angiogenesis by targeting VHL and is associated with poor prognosis and triple-negative breast cancer. *Oncogene*, 2014; 33: 679-89
9. Tekiner TA, Basaga H: Role of microRNA deregulation in breast cancer cell chemoresistance and stemness. *Curr Med Chem*, 2013; 20: 3358-69
10. Liu ZL, Wang H, Liu J, Wang ZX: MicroRNA-21 (miR-21) expression promotes growth, metastasis, and chemo- or radioresistance in non-small cell lung cancer cells by targeting PTEN. *Mol Cell Biochem*, 2013; 372: 35-45
11. Grosso S, Doyen J, Parks SK et al: MiR-210 promotes a hypoxic phenotype and increases radioresistance in human lung cancer cell lines. *Cell Death Dis*, 2013; 4: e544
12. Lee KM, Choi EJ, Kim IA: microRNA-7 increases radiosensitivity of human cancer cells with activated EGFR-associated signaling. *Radiother Oncol*, 2011; 101: 171-76
13. Liao H, Xiao Y, Hu Y et al: microRNA-32 induces radioresistance by targeting DAB2IP and regulating autophagy in prostate cancer cells. *Oncol Lett*, 2015; 10: 2055-62
14. Li G, Liu Y, Su Z et al: MicroRNA-324-3p regulates nasopharyngeal carcinoma radioresistance by directly targeting WNT2B. *Eur J Cancer*, 2013; 49: 2596-607
15. Li G, Wang Y, Liu Y et al: miR-185-3p regulates nasopharyngeal carcinoma radioresistance by targeting WNT2B *in vitro*. *Cancer Sci*, 2014; 105: 1560-68
16. Qu C, Liang Z, Huang J et al: MiR-205 determines the radioresistance of human nasopharyngeal carcinoma by directly targeting PTEN. *Cell Cycle*, 2012; 11: 785-96
17. Yong FL, Law CW, Wang CW: Potentiality of a triple microRNA classifier: miR-193a-3p, miR-23a and miR-338-5p for early detection of colorectal cancer. *BMC Cancer*, 2013; 13: 280
18. Yates M, Cheong E, Luben R et al: Body mass index, smoking, and alcohol and risks of Barrett's esophagus and esophageal adenocarcinoma: A UK prospective cohort study. *Dig Dis Sci*, 2014; 59: 1552-59
19. Avci CB, Harman E, Dodurga Y et al: Therapeutic potential of an anti-diabetic drug, metformin: Alteration of miRNA expression in prostate cancer cells. *Asian Pac J Cancer Prev*, 2013; 14: 765-68
20. Deng H, Lv L, Li Y et al: miR-193a-3p regulates the multi-drug resistance of bladder cancer by targeting the LOXL4 gene and the oxidative stress pathway. *Mol Cancer*, 2014; 13: 234
21. Lin YM, Chu PH, Li YZ, Ouyang P: Ribosomal protein pN040 mediates nucleolar sequestration of SR family splicing factors and its overexpression impairs mRNA metabolism. *Cell Signal*, 2017; 32: 12-23
22. Edmond V, Merdzhanova G, Gout S et al: A new function of the splicing factor SRSF2 in the control of E2F1-mediated cell cycle progression in neuroendocrine lung tumors. *Cell Cycle*, 2013; 12: 1267-78
23. Kedzierska H, Poplawski P, Hoser G et al: Decreased expression of SRSF2 splicing factor inhibits apoptotic pathways in renal cancer. *Int J Mol Sci*, 2016; 17: pii: E1598

The present study shows that miR-193a-3p is also involved in the radio-resistance of NPC. A comparative expression analysis of miR-193a-3p was conducted, showing that the SRSF2 gene is correlated negatively with radio-resistance (Figure 3). The mechanisms and roles of SRSF2 and miR-193a-3p in radio-resistance of NPC have been systematically demonstrated in cultured cells.

Expression of SRSF2 is clearly involved in radio-resistance in NPC cell lines, and this action is mediated by miR-193a-3p. Nevertheless, further research is needed to define the mechanism by which miR-193a-3p mediates SRSF2 repression in NPC.

## Conclusions

miR-193a-3p can regulate the radio-resistance of nasopharyngeal cancer, possibly through control of the hypoxia signaling pathway and its target gene, SRSF2. miR-193a-3p might function as an underlying biomarker for nasopharyngeal cancer radio-resistance.

## Conflict of interests

None.

24. Li J, Tu Z, Shen Z et al: Quantitative measurement of optical attenuation coefficients of cell lines CNE1, CNE2, and NP69 using optical coherence tomography. *Lasers Med Sci*, 2013; 28: 621–25
25. Lv L, Deng H, Li Y et al: The DNA methylation-regulated miR-193a-3p dictates the multi-chemoresistance of bladder cancer via repression of SRSF2/PLAU/HIC2 expression. *Cell Death Dis*, 2014; 5: e1402
26. Deng H, Lv L, Li Y et al: The miR-193a-3p regulated PSEN1 gene suppresses the multi-chemoresistance of bladder cancer. *Biochim Biophys Acta*, 2015; 1852: 520–28
27. Oh JS, Kim JJ, Byun JY, Kim IA: Lin28-let7 modulates radiosensitivity of human cancer cells with activation of K-Ras. *Int J Radiat Oncol Biol Phys*, 2010; 76: 5–8
28. Wang P, Zhang J, Zhang L et al: MicroRNA 23b regulates autophagy associated with radioresistance of pancreatic cancer cells. *Gastroenterology*, 2013; 145: 1133–43e12
29. Zhang Y, Zheng L, Huang J et al: MiR-124 Radiosensitizes human colorectal cancer cells by targeting PRRX1. *PLoS One*, 2014; 9: e93917
30. McFarlane M, MacDonald AI, Stevenson A, Graham SV: Human Papillomavirus 16 oncoprotein expression is controlled by the cellular splicing factor SRSF2 (SC35). *J Virol*, 2015; 89: 5276–87